Adaptive optics compensation of multiple orbital angular momentum beams propagating through emulated atmospheric turbulence

Yongxiong Ren,[1,*] Guodong Xie,[1] Hao Huang,[1] Changjing Bao,[1] Yan Yan,[1] Nisar Ahmed,[1] Martin P. J. Lavery,[2] Baris I. Erkmen,[3,8] Samuel Dolinar,[3] Moshe Tur,[4] Mark A. Neifeld,[5] Miles J. Padgett,[2] Robert W. Boyd,[6] Jeffrey H. Shapiro,[7] and Alan E. Willner[1]

[1]*Department of Electrical Engineering, University of Southern California, Los Angeles, California 90089, USA*

[2]*School of Physics and Astronomy, University of Glasgow, Glasgow, G12 8QQ, UK*

[3]*Jet Propulsion Laboratory, California Institute of Technology, Pasadena, California 91109, USA*

[4]*School of Electrical Engineering, Tel-Aviv University, Tel-Aviv 69978, Israel*

[5]*Department of Electrical and Computer Engineering, University of Arizona, Tucson, Arizona 85721, USA*

[6]*Department of Physics and Astronomy, The Institute of Optics, University of Rochester, Rochester, New York 14627, USA*

[7]*Massachusetts Institute of Technology, Research Laboratory of Electronics, Cambridge, Massachusetts 02139, USA*

[8]*Baris I. Erkmen is currently with Google Inc., Mountain View, California, USA*

**Corresponding author: yongxior@usc.edu*

Received February 6, 2014; revised April 7, 2014; accepted April 7, 2014;
posted April 8, 2014 (Doc. ID 204794); published May 5, 2014

We propose an adaptive optics compensation scheme to simultaneously compensate multiple orbital angular momentum (OAM) beams propagating through atmospheric turbulence. A Gaussian beam on one polarization is used to probe the turbulence-induced wavefront distortions and derive the correction pattern for compensating the OAM beams on the orthogonal polarization. By using this scheme, we experimentally demonstrate simultaneous compensation of multiple OAM beams, each carrying a 100 Gbit/s data channel through emulated atmospheric turbulence. The experimental results indicate that the correction pattern obtained from the Gaussian probe beam could be used to simultaneously compensate multiple turbulence-distorted OAM beams with different orders. It is found that the turbulence-induced crosstalk effects on neighboring modes are efficiently reduced by 12.5 dB, and the system power penalty is improved by 11 dB after compensation.

OCIS codes: (010.1080) Active or adaptive optics; (010.1330) Atmospheric turbulence; (060.2605) Free-space optical communication; (060.4230) Multiplexing.
http://dx.doi.org/10.1364/OL.39.002845

Multiplexing techniques for multiple data channels, such as wavelength-division multiplexing, have been widely used to enhance data capacity in optical communication systems. Recently, another potential technique that has gained much attention is space division multiplexing (SDM), in which separable spatial modes carry independent data streams to increase system capacity and spectral efficiency [1,2]. One of the promising approaches in SDM is to multiplex orbital-angular-momentum (OAM) carrying beams [1–4].

Light beams carrying OAM are characterized by their $\exp(il\varphi)$ $(l = 0, \pm 1, \pm 2, \ldots)$ azimuthal phase structures, in which φ refers to the azimuth angle and l determines the OAM charge [5]. One key characteristic of OAM beams is that modes with different l (l can take any integer value) are orthogonal to one another [5,6]. Therefore, multiple OAM beams each carrying an independent data stream can be multiplexed at a transmitter and demultiplexed at a receiver [1–3].

Several reports have shown that OAM multiplexing can be used in free-space optical (FSO) links to significantly enhance data capacity and spectral efficiency [1,7]. For example, multiplexing 32 OAM beams has been demonstrated in an FSO link, providing a total 2.56 Tbit/s capacity and 95.7 bits/s/Hz efficiency [1]. However, a critical limitation of OAM-based FSO systems is the significant performance degradations induced by atmospheric turbulence [8,9]. As the orthogonality of multiple co-propagating OAM beams depends on their distinct helical phase-fronts, the refractive index inhomogeneities of the atmosphere will distort these phase-fronts, causing power spreading of each transmitted OAM mode onto neighboring modes, which will essentially result in intermodal crosstalk between different OAM data channels [8–12].

An important goal for future use of OAM in high-capacity SDM-based FSO links might be the ability to compensate the effects of atmospheric turbulence [8,9]. Figure 1 illustrates this concept. Two technical challenges must be overcome for turbulence compensation of OAM beams: (a) the conventional Shack–Hartmann wavefront sensing technique cannot be readily used for reconstructing the helical phase-front of the OAM

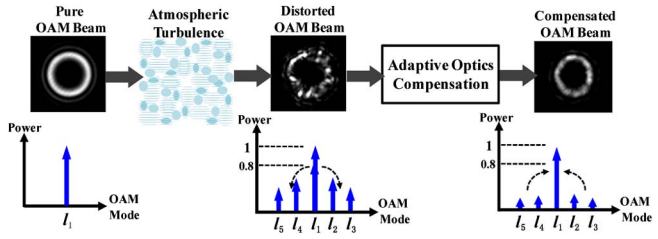

Fig. 1. Conceptual diagram for turbulence compensation of a distorted OAM beam. The adaptive-optics compensation system reduces power leakage to neighboring modes caused by atmospheric turbulence.

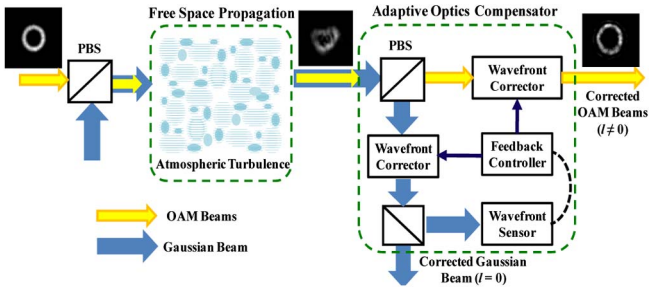

Fig. 2. Scheme for turbulence compensation of multiple OAM beams using a Gaussian probe beam for wavefront sensing. PBS, polarizing beam splitter.

beam, due to its phase singularities or branch points caused by turbulence [13–15]; and (b) the receiver's turbulence compensation system must correct multiple independent OAM beams simultaneously.

In this Letter, we describe an adaptive optics (AO) compensation scheme that corrects multiple turbulence-distorted OAM beams by using a Gaussian beam (i.e., $l = 0$) as a probe beam for wavefront sensing. Using this scheme, we demonstrate simultaneous turbulence compensation of multiple OAM beams, each carrying a 100 Gbit/s data channel [16]. A rotating phase screen plate with a pseudo-random phase distribution obeying Kolmogorov spectrum statistics [13] is used to emulate atmospheric turbulence in the laboratory environment [9].

Our scheme for simultaneous compensation of multiple OAM beams is shown in Fig. 2. Multiplexed OAM beams ($l \neq 0$) on one polarization are combined with an orthogonally polarized Gaussian beam ($l = 0$) using a polarizing beam splitter (PBS). The resulting beams propagate collinearly through emulated atmospheric turbulence. At the receiver side, an AO compensation system is built, in which the distorted Gaussian beam is separated from the distorted OAM beams using another PBS to serve as the probe for wavefront distortion estimations and required correction-pattern retrieval. A feedback controller is used to update the two wavefront correctors with the same correction pattern obtained to compensate the phase-front of the Gaussian probe, as well as those of the distorted OAM beams. As the polarization of a laser beam propagating through the turbulence is highly preserved [13, 17], the depolarization effect on the beams is negligible.

The experimental implementation of the proposed scheme is presented in Fig. 3. The 100 Gbit/s quadrature phase-shift keying (QPSK) signal generated by the QPSK transmitter is split into three copies, each of which is decorrelated using single-mode fibers (SMFs) with different lengths. The three signal copies are sent to three collimators, each of which converts the output of the SMF to a collimated Gaussian beam with a beam diameter of 3 mm. One beam (branch ①) is launched onto a reflective spatial light modulator (SLM-1) loaded with a specific blazed-fork hologram to create one OAM beam. Another beam (branch ②) is converted into a superposition of two equally weighted OAM beams (with OAM charges of $l = 3, 7$) by loading SLM-2 with a specially designed phase hologram [18]. The SLMs used here are polarization dependent liquid-crystal-based reflective phase modulators with a spatial resolution of 20 μm. Branch ② is only turned on when investigating the impact of OAM crosstalk on the average bit-error-rate (BER) of the multiplexed OAM channels. The other Gaussian beam (branch ③) is polarization rotated using a half-wave plate (HWP-1) and then expanded using a 4-f lens system to become as wide as the widest OAM beam (i.e., $l = 9$ in this experiment) along the propagation path. This branch is then polarization multiplexed with branches ① and ② via a PBS. The resulting multiplexed beams are sent through the atmospheric turbulence emulator [9].

The effects of turbulence are emulated by a thin phase screen plate that is mounted on a rotatable stage and placed in the middle of the optical path. A pseudo-random phase distribution obeying Kolmogorov spectrum statistics and characterized by its effective Fried coherence length r_0 was machined into the plate [19,20]. The r_0 of the phase screen plate is 1 mm, which in our case could represent weak-to-moderate turbulence over a 1 km link distance [9,21].

The beam exiting from the turbulence emulator is imaged onto the wavefront corrector (SLM-3) using a 4-f lens system. For simplification, only one wavefront corrector (i.e., SLM-3) is used in the AO compensation system, which is shared when compensating the

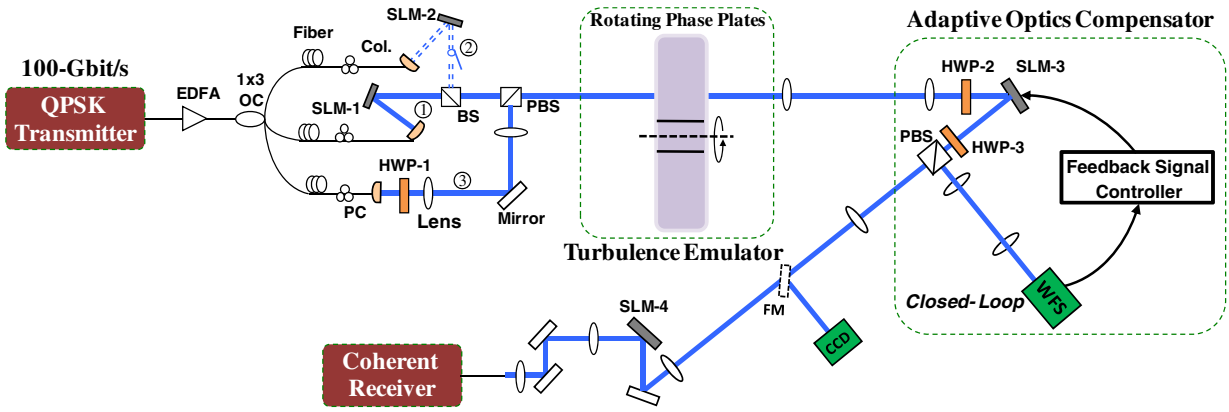

Fig. 3. Experimental setup. BS: beam splitter, Col.: Collimator, EDFA: erbium-doped fiber amplifier, FM: flip mirror, HWP: half-wave plate, OC: optical coupler, PBS: polarization beam splitter, PC: polarization controller, QPSK: quadrature phase shift keying, SLM: spatial light modulator, WFS: wavefront sensor.

Gaussian beam and the OAM beams for one turbulence realization. As the adopted SLM is polarization sensitive, HWP-2 is used to align the polarization of the Gaussian probe beam with the polarization orientation of SLM-3. The beams after SLM-3 are also polarization adjusted by HWP-3 to ensure that the Gaussian beam is directed to the wavefront sensor. Similarly, the plane of SLM-3 is imaged onto the plane of the Shack–Hartmann wavefront sensor (WFS, HASO from Imagine Optic Inc.), which enables the WFS to detect the residual wavefront distortion of the Gaussian probe beam. A feedback controller is used to communicate between SLM-3 and WFS and provide the correction pattern as a control signal. Once the loop converges and the ultimate correction pattern is obtained for this turbulence realization, HWP-2 is then rotated by 90° to align the polarization of OAM beams with the polarization orientation of SLM-3. By doing so, the OAM beams rather than the Gaussian beam will be phase corrected by SLM-3.

After the AO system, a CCD camera captures the far-field intensity profile of the corrected beam, followed by an SLM-based demultiplexer for BER measurement. In order to reduce the effect of turbulence-induced tilt/tip on OAM demultiplexing, the beam exiting from SLM-3 is imaged onto SLM-4. By loading an inverse spiral phase hologram of the OAM channel to be detected onto SLM-4, the OAM beam is subsequently converted into a Gaussian beam. This Gaussian beam is then coupled into an SMF and sent for coherent detection and off-line signal processing.

Figure 4 shows the intensity profiles of the Gaussian probe and OAM beams for a particular turbulence realization with and without compensation. With the AO system, the root mean square wavefront error and Strehl ratio of the Gaussian beam are improved from 0.613, 0.234 to 0.092, 0.924, respectively. The correction pattern obtained from the Gaussian probe beam is used to compensate the OAM beams (from branch ①). From the far-field images, one can see that the distorted OAM beams (upper), up to OAM charge $l = 9$, are corrected. As OAM beams have different beam sizes, they experience different turbulence strengths, which are characterized by D/r_0, with D being the beam diameter at the turbulence emulator plane. It is expected that using the same correction pattern, lower-order OAM beams will experience better compensation, as shown in Fig. 4.

To further examine compensation performance, Fig. 5(a) shows the crosstalk (the received power of OAM channel $l = 6$ or 7 divided by the received power of channel $l = 5$) with and without compensation for

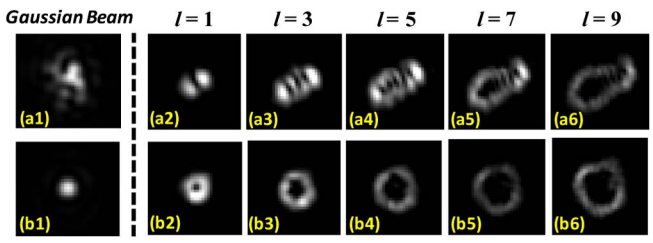

Fig. 4. Far-field intensity images of the Gaussian probe beam and OAM beams ($l = 1, 3, 5, 7, 9$) before [upper, (a1)–(a6)] and after [lower, (b1)–(b6)] compensation.

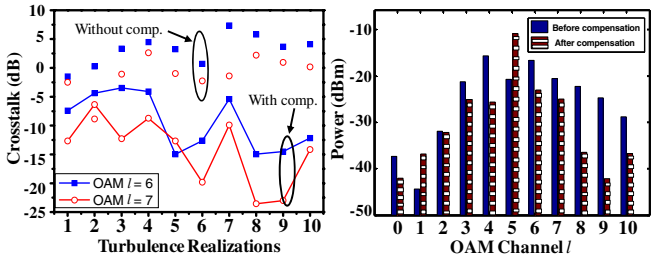

Fig. 5. (a) Crosstalk of OAM channel $l = 5$ onto adjacent channels $l = 6$ and 7 for 10 different turbulence realizations. (b) Power distribution (coupled into an SMF) of different OAM channels when transmitting OAM $l = 5$ with and without compensation for turbulence realization #10.

10 different turbulence realizations. We observe that using the correction pattern obtained from the Gaussian probe beam, the crosstalk of OAM $l = 5$ onto adjacent channels $l = 6$, 7 are decreased by about 12.5 and 13.2 dB, respectively. Here the positive crosstalk value is caused primarily by the turbulence-induced tilt/tip, which are the dominant terms in the wavefront error before being corrected by the AO system. Figure 5(b) presents the distribution of power coupled into the fiber when transmitting OAM channel $l = 5$ with and without compensation. We see that without compensation, the power is spread among neighboring modes, whereas with compensation, the received power is better confined to the OAM channel $l = 5$.

Figure 6 shows the BER performance when only one OAM channel ($l = 1$, 3, 5, or 7) is transmitted with and without compensation for various turbulence realizations. For fair comparison, the received power of each channel after compensation over 10 different turbulence realizations is maintained to be around –34 dBm. We see that the BERs for these OAM channels are improved by compensation, with all being below the forward error correction (FEC) limit. The lower-order OAM channels have better BER performance, due to the fact that lower-order OAM beams experience smaller turbulence distortions as their beam sizes increase slower than those of the higher-order OAM beams.

To illustrate the system power penalty improvement provided by the proposed compensation approach, we measure the average BER of OAM channel $l = 5$ (from

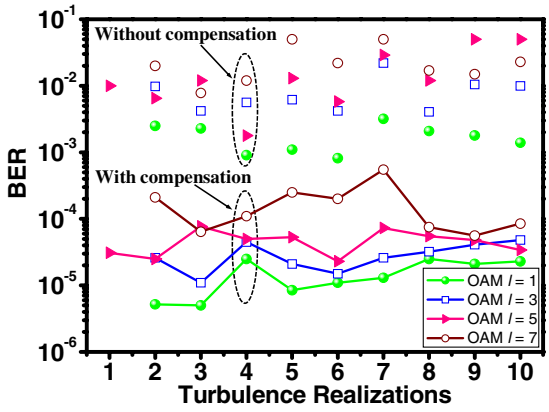

Fig. 6. BER for different OAM channels ($l = 1$, 3, 5, or 7) with and without compensation.

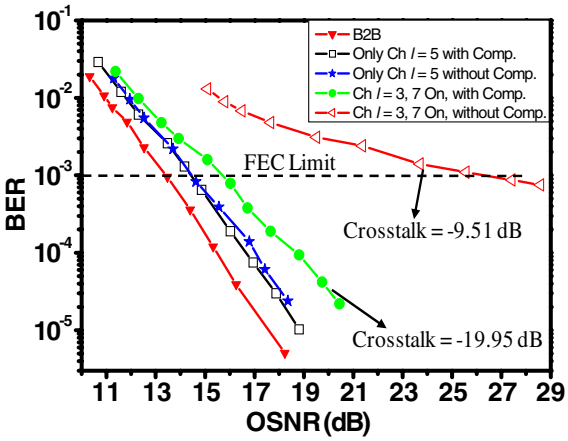

Fig. 7. BERs for OAM channel $l = 5$ when transmitting three OAM channels $l = 3, 5, 7$ with and without compensation for turbulence realization #10.

branch ①) for a fixed turbulence realization. To introduce crosstalk effects from the neighboring channels, branch ② is turned on, and three OAM multiplexed channels $l = 3, 5, 7$ are transmitted (note that channels $l = 3, 7$ transmit the same data). Figure 7 presents the BER curves as a functions of optical signal-to-noise ratio (OSNR) for OAM channel $l = 5$ with and without compensation. We see that the BER curve without compensation when all OAM channels are on, exhibits an error floor, which is due to the severe crosstalk. The measured crosstalk from OAM channels $l = 3$ and $l = 7$ to channel $l = 5$ is reduced from −9.51 to −19.95 dB by compensation. Meanwhile, the power penalty is improved by 11 dB after compensation at FEC limit of BER $= 1 \times 10^{-3}$.

In conclusion, an adaptive optics compensation approach for an OAM multiplexed FSO communication system is described, in which a Gaussian beam is used to probe the turbulence-induced wavefront distortions and derive the correction pattern for compensating the OAM beams. Using this approach, we experimentally demonstrate simultaneous compensation of multiple OAM beams, each carrying a 100 Gbit/s data channel through emulated atmospheric turbulence. The experimental results show that the proposed scheme can efficiently compensate OAM beams with OAM order up to $l = 9$. After compensation, the turbulence-induced crosstalk to neighboring modes of OAM $l = 5$ is reduced by 12.5 dB, and the power penalty of OAM channel $l = 5$ is improved by 11 dB.

We acknowledge Jerome Ballesta from Imagine Optic Inc. for helpful discussions. Our work is supported by DARPA under the InPho program.

References

1. J. Wang, J.-Y. Yang, I. M. Fazal, N. Ahmed, Y. Yan, H. Huang, Y. Ren, Y. Yue, S. Dolinar, M. Tur, and A. E. Willner, Nat. Photonics **6**, 488 (2012).
2. N. Bozinovic, Y. Yue, Y. Ren, M. Tur, P. Kristensen, H. Huang, A. E. Willner, and S. Ramachandran, Science **340**, 1545 (2013).
3. G. Gibson, J. Courtial, M. J. Padgett, M. Vasnetsov, V. Pas'ko, S. Barnett, and S. Franke-Arnold, Opt. Express **12**, 5448 (2004).
4. T. Su, R. P. Scott, S. S. Djordjevic, N. K. Fontaine, D. J. Geisler, X. Cai, and S. J. B. Yoo, Opt. Express **20**, 9396 (2012).
5. L. Allen, M. W. Beijersbergen, R. J. C. Spreeuw, and J. P. Woerdman, Phys. Rev. A **45**, 8185 (1992).
6. A. Yao and M. Padgett, Adv. Opt. Photon. **3**, 161 (2011).
7. H. Huang, G. Xie, Y. Yan, N. Ahmed, Y. Ren, Y. Yue, D. Rogawski, M. J. Willner, B. I. Erkmen, K. M. Birnbaum, S. J. Dolinar, M. P. J. Lavery, M. J. Padgett, M. Tur, and A. E. Willner, Opt. Lett. **39**, 197 (2014).
8. B. Rodenburg, M. P. J. Lavery, M. Malik, M. N. O'Sullivan, M. Mirhosseini, D. J. Robertson, M. J. Padgett, and R. W. Boyd, Opt. Lett. **37**, 3735 (2012).
9. Y. Ren, H. Huang, G. Xie, N. Ahmed, B. Erkmen, N. Chandrasekaran, M. P. J. Lavery, J. Shapiro, N. Steinhoff, M. Tur, M. J. Padgett, R. W. Boyd, and A. E. Willner, Opt. Lett. **38**, 4062 (2013).
10. J. A. Anguita, M. A. Neifeld, and B. V. Vasic, Appl. Opt. **47**, 2414 (2008).
11. C. Paterson, Phys. Rev. Lett. **94**, 153901 (2005).
12. N. Chandrasekaran and J. H. Shapiro, J. Lightwave Technol. **32**, 1075 (2014).
13. L. Andrews and R. Phillips, *Laser Beam Propagation Through Random Media*, 2nd ed. (SPIE, 2005).
14. K. Murphy, D. Burke, N. Devaney, and C. Dainty, Opt. Express **18**, 15448 (2010).
15. C. Huang, H. Huang, H. Toyoda, T. Inoue, and H. Liu, Opt. Express **20**, 26099 (2012).
16. Y. Ren, G. Xie, H. Huang, C. Bao, Y. Yan, N. Ahmed, M. P. J. Lavery, B. Erkmen, S. Dolinar, M. Tur, M. Neifeld, M. J. Padgett, R. W. Boyd, J. H. Shapiro, and A. E. Willner, in *European Conference on Optical Communication (ECOC)* (2013), paper We.3.D.1.
17. M. Toyoshima, H. Takenaka, Y. Shoji, Y. Takayama, Y. Koyama, and H. Kunimori, Opt. Express **17**, 22333 (2009).
18. J. Leach, M. R. Dennis, J. Courtial, and M. J. Padgett, New J. Phys. **7**, 55 (2005).
19. K. L. Baker, E. A. Stappaerts, D. Gavel, S. C. Wilks, J. Tucker, D. A. Silva, J. Olsen, S. S. Olivier, P. E. Young, M. W. Kartz, L. M. Flath, P. Krulevitch, J. Crawford, and O. Azucena, Appl. Opt. **43**, 5585 (2004).
20. P. Polynkin, A. Peleg, L. Klein, T. Rhoadarmer, and J. Moloney, Opt. Lett. **32**, 885 (2007).
21. L. Andrews, R. Phillips, and A. R. Weeks, Wave Random Media **7**, 229 (1997).